AIP Applied Physics Letters

Growth mode and structural characterization of GaSb on Si (001) substrate: A transmission electron microscopy study

Y. H. Kim, J. Y. Lee, Y. G. Noh, M. D. Kim, S. M. Cho et al.

Citation: Appl. Phys. Lett. 88, 241907 (2006); doi: 10.1063/1.2209714
View online: http://dx.doi.org/10.1063/1.2209714
View Table of Contents: http://apl.aip.org/resource/1/APPLAB/v88/i24
Published by the American Institute of Physics.

Additional information on Appl. Phys. Lett.

Journal Homepage: http://apl.aip.org/
Journal Information: http://apl.aip.org/about/about_the_journal
Top downloads: http://apl.aip.org/features/most_downloaded
Information for Authors: http://apl.aip.org/authors

ADVERTISEMENT

Downloaded 21 Apr 2013 to 143.248.118.122. This article is copyrighted as indicated in the abstract. Reuse of AIP content is subject to the terms at: http://apl.aip.org/about/rights_and_permissions

Growth mode and structural characterization of GaSb on Si (001) substrate: A transmission electron microscopy study

Y. H. Kim and J. Y. Lee[a)]
Department of Materials Science and Engineering, Korea Advanced Institute of Science and Technology, Daejeon 305-701, Republic of Korea

Y. G. Noh and M. D. Kim
Department of Physics, Chungnam National University, Daejeon 220, Republic of Korea

S. M. Cho, Y. J. Kwon, and J. E. Oh
Division of Electrical and Computer Engineering, Hanyang University, Ansan 425-791, Republic of Korea

(Received 9 January 2006; accepted 21 April 2006; published online 13 June 2006)

Growth mode and structural properties of GaSb layers grown on silicon substrate by molecular beam epitaxy method are investigated by transmission electron microscopy. It is found that the GaSb grows to three-dimensional islands and grains are tilted to reduce a lattice mismatch through twin boundaries when they are directly grown on Si substrate. A low-temperature (LT) AlSb buffer plays a key role in transferring the growth mode from a three-dimensional island to a layer-by-layer structure. When the LT AlSb layer is used as a buffer, 90° misfit dislocations, with the Burgers vector **b** of $1/2a\,\langle 110\rangle$, are observed on the interface. © *2006 American Institute of Physics*.
[DOI: 10.1063/1.2209714]

Epitaxial growth of III–V compound semiconductors on silicon (Si) substrate has several advantages, including its high quality, large area, and low cost compared with substrates of compound semiconductors. In addition, this process makes possible the large scale integration of compound semiconductors for optical and electronic devices. Therefore, a lot of effort has been concentrated on growing compound semiconductors, mostly arsenides or nitrides, on Si substrates.

In comparison with other III-V compound semiconductors, studies of III-Sb based compound semiconductors on Si substrate have been insufficient. The III-Sb based compound semiconductors have recently attracted a lot of attention due to their high performance in devices.[1–7] Specially, gallium antimonide (GaSb) is considered a key substrate material because its lattice parameter matches solid solutions of various ternary and quaternary III–V compounds whose band gaps cover a wide range from 0.17 eV of InSb to 1.58 eV of AlSb.[8] GaSb based structures have potential applications in laser diodes with low threshold voltage,[9,10] photodetectors with high quantum efficiency,[11–13] high frequency devices,[14,15] superlattice with tailored optical and transport characteristics,[16] and booster cells in tandem solar cell arrangement for improved efficiency of photovoltaic cells.[17] In addition, because of its band structural properties, GaSb has been considered an ideal material for the study of the Auger recombination.[18]

However, the growth of III-Sb based compound semiconductors on silicon substrate presents several fundamental problems. First, the large difference in lattice constants and thermal expansion coefficients of the layers can produce misfit dislocations and stress in the epitaxial films. Second, the growth of polar compounds on nonpolar substrates can lead to antiphase domains. The report by Akahane *et al.* is one of the few studies on the heteroepitaxial growth of GaSb on Si substrate. They introduced an AlSb initiation layer for the heteroepitaxy of GaSb.[4]

In this letter, we report the growth modes and the dependence on a buffer of GaSb layers. We have observed that the structural properties of GaSb layer can be dramatically changed by inserting low-temperature (LT) AlSb buffer as suggested by Akahane *et al.*[4] and Balakrishnan *et al.*[19,20] Specifically, this letter shows the crystallographic relation between GaSb and Si substrate and the change of growth modes by insertion of a specified buffer layer characterized by transmission electron microscopy (TEM).

GaSb layers have been grown by molecular beam epitaxy (MBE). In this study, Riber 32-PMBE system with effusion cells for the III sources and the dual filament cell for the antimony (Sb) source was used to synthesize compound semiconductors. *p*-type Si (001) wafers were used as substrate. The Si substrate was pretreated to remove an alien substance on the surface and loaded into the chamber. The Si substrate was heated for 30 min at 900 °C for deoxidation in the chamber. Then the Sb was soaked on the Si substrate for 5 min.

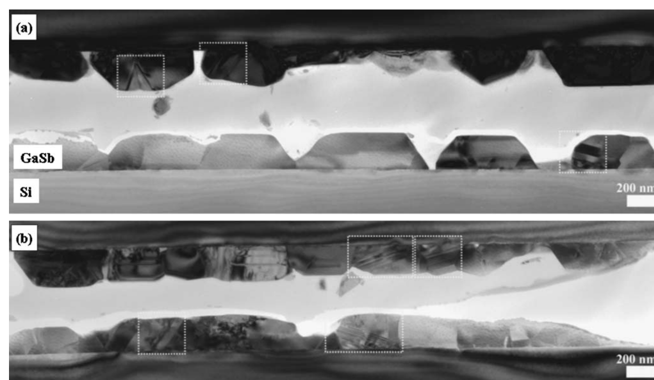

FIG. 1. Cross-sectional TEM micrograph taken from sample A (GaSb directly grown on Si substrate). (a) Island growth. (b) Coalescence of islands.

a)Author to whom correspondence should be addressed; electronic mail: j.y.lee@kaist.ac.kr

 © 2006 American Institute of Physics

Downloaded 21 Apr 2013 to 143.248.118.122. This article is copyrighted as indicated in the abstract. Reuse of AIP content is subject to the terms at: http://apl.aip.org/about/rights_and_permissions

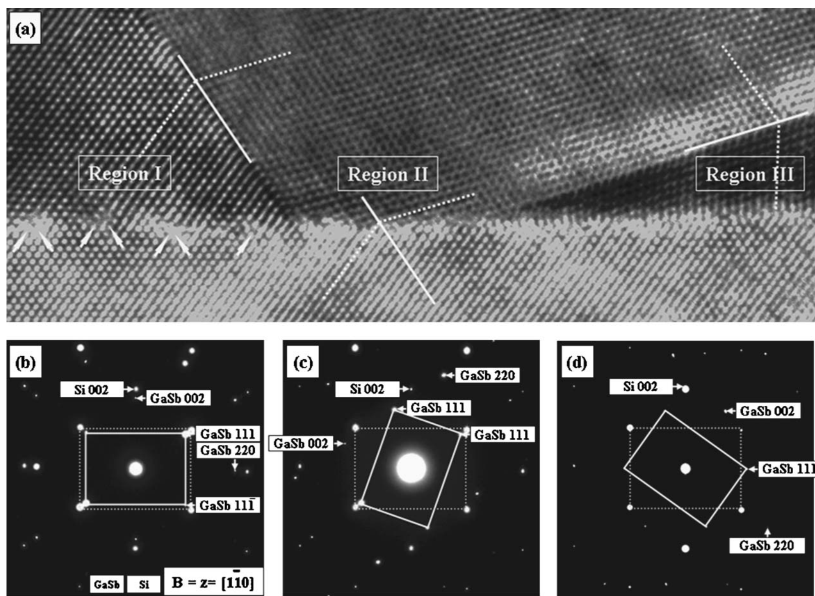

FIG. 2. (a) Cross-sectional high-resolution TEM (HRTEM) micrograph for sample A through $[1\bar{1}0]$ zone axis. (b) Selected area electron diffraction (SAED) pattern taken between region I and Si substrate. (c) SAED pattern taken between region II and Si substrate. (d) SAED pattern taken between region III and Si substrate. The zone axis of all of the SAED patterns is indexed as $[1\bar{1}0]$ of zinc-blende structure.

Two GaSb layers with different structures were grown to study the growth mode and buffer dependence of GaSb layers. In one sample (sample A), GaSb was directly grown on Si substrate. The GaSb layer was grown to 250 nm in thickness at the growth rate of 5 nm/min. The V/III flux ratio for the GaSb was close to 8.5.

In the other sample (sample B), the LT AlSb buffer was inserted between GaSb and Si substrate. The LT AlSb buffer was deposited with a thickness of 8 monolayers (ML) at 1 ML/s. The V/III flux ratio for the AlSb was kept at 8.

In this study, growth mode and structural properties were studied with TEM micrographs and selected area electron diffraction (SAED) patterns recorded with JEOL-2000EX and JEOL-3010 TEMs. Specially, the orientation relationships between layers were deeply treated using TEM.

Figure 1 shows the cross-sectional micrographs of the GaSb directly grown on Si substrate. The growth stages in Figs. 1(a) and 1(b) are the three-dimensional (3D) GaSb islands and their coalescences, respectively. The height of the island is about 250 nm in Figs. 1(a) and 1(b). A lot of planar defects are shown in Fig. 1 (the rectangular boxes show planar defects).

Figure 2 shows an important high-resolution TEM (HRTEM) micrograph and SAED patterns of the interface between the GaSb and Si substrate. Two twin boundaries are shown in the GaSb layer of Fig. 2(a), respectively, between region I and region II and between region II and region III. A few misfit dislocations were found on the interface between the GaSb of region I and Si substrate (the arrows indicate the misfit dislocations). A similar relationship to twin boundary was observed between the GaSb of region II and Si substrate. Figure 2(b) is a SAED pattern taken between the GaSb of region I and Si substrate. The relative orientation between the GaSb of region I and Si substrate in Fig. 2(a) is the GaSb$\langle 110\rangle \| Si\langle 110\rangle$ and GaSb$\{002\}\|$Si$\{002\}$ [Fig. 2(b)]. The SAED pattern in Fig. 2(c) shows that the $11\bar{1}$ plane of GaSb is parallel to the (111) plane of Si, which is similar to the twin relationship. The (111) plane of GaSb in region III is parallel to the (220) plane of Si substrate in Fig. 2(a), which is well proved by the SAED pattern of Fig. 2(d). Analysis of the SAED patterns shows that the GaSb of region II is in a twin relation with the GaSb of region I and region III.

Figure 3 shows the HRTEM micrograph with the relative orientation of GaSb$\langle 110\rangle \|$Si$\langle 110\rangle$ and GaSb$\{111\}\|$Si$\{220\}$. Figures 3(b) and 3(c) are the fast Fourier transformation (FFT) and the inverse fast Fourier transformation (IFFT) results carried out for an extended structural study. The FFT image of Fig. 3(b) is exactly alike the SAED pattern of Fig. 2(d). The zone axis is indexed as $[1\bar{1}0]$ and the GaSb (111) plane is parallel to the Si (220) plane in both the FFT image

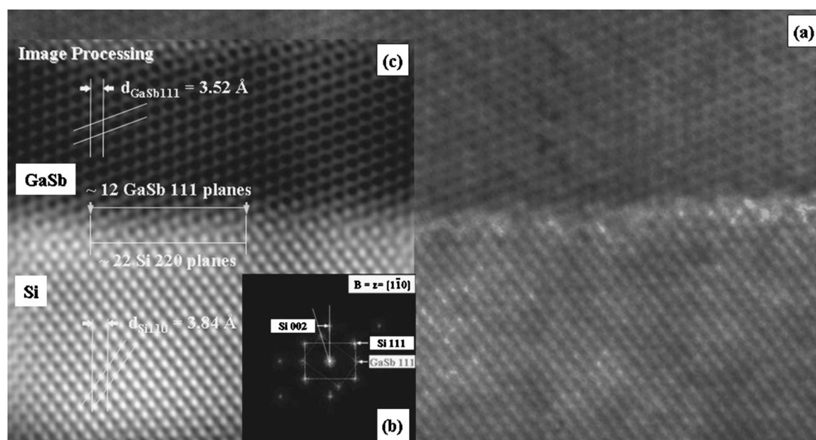

FIG. 3. (a) HRTEM micrograph with the relative orientation of GaSb $\langle 110\rangle \|$Si$\langle 110\rangle$ and GaSb $\{111\}\|$Si$\{220\}$. [(b) and (c)] Fast Fourier transformation (FFT) and inverse fast Fourier transformation (IFFT) results carried out for an extended structural study, respectively. The FFT and the IFFT results well demonstrate the orientation relationship at the GaSb/Si interface. Specifically, the IFFT image clearly shows the interplanar spacing relationship between the GaSb and the Si substrate.

Downloaded 21 Apr 2013 to 143.248.118.122. This article is copyrighted as indicated in the abstract. Reuse of AIP content is subject to the terms at: http://apl.aip.org/about/rights_and_permissions

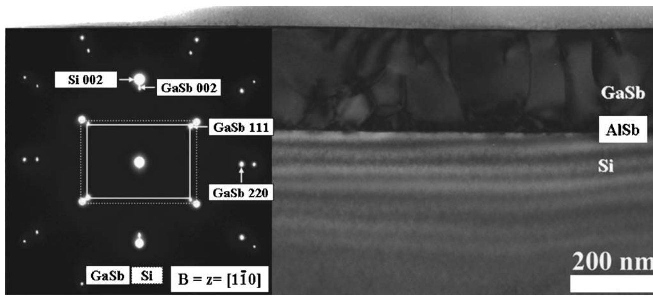

FIG. 4. Cross-sectional TEM micrograph taken from sample B. The index of zone axis of the SAED pattern is.[1$\bar{1}$0]

and Fig. 3(b). In this case, the misfit δ between the GaSb layer and Si substrate is defined by

$$\delta=(2d_{\mathrm{Si}\ 220}-d_{\mathrm{GaSb}\ 111})/d_{\mathrm{GaSb}\ 111}=0.091.$$

This value is smaller than the misfit δ' of the system with the relative orientation of GaSb$\langle 110\rangle \| Si\langle 110\rangle$ and GaSb$\{002\}\|$Si$\{002\}$ ($\delta' = \sim 0.122$). If extra half planes are introduced into the structure for strain relaxation, the average spacing S of misfit dislocations depends on the misfit δ and is of the order of $(2d_{\mathrm{Si}\ 220})/\delta$. Therefore the S is determined in Fig. 3(c) as follows:

$$S=(2)(1.92)/0.091=42.2\ \text{Å}=4.22\ \text{nm}.$$

Because the interplanar spacings of (220) planes of the Si substrate and that of (111) planes of the GaSb are about 1.92 and 3.52 Å, the (220) plane of Si and the (111) plane of the GaSb must accord with each other about every 12 planes for GaSb and 22 planes for Si. Figure 3(c) demonstrates this result. From the above results, the crystallographic orientation relation was changed through twin boundaries with (111) plane as mirror plane to reduce the lattice misfit between GaSb and the Si substrate when the GaSb was directly grown on Si substrate.

The LT AlSb buffer layer plays a critical role for improving the crystallinity of the GaSb layer in the growth process of GaSb on Si substrate.

Figure 4 shows the cross-sectional TEM micrograph and SAED pattern for the GaSb grown on the LT AlSb buffer layer deposited after antimony (Sb) soaking. The introduction of the AlSb buffer layer clearly improved the quality of the GaSb crystals. The GaSb layer has very flat surfaces and interfaces. The dislocations are mostly generated near the interface between the GaSb layer and Si substrate, and the dislocation density decreases with the increase of the thickness of the GaSb layer. The SAED pattern shows the relative orientation of the GaSb$\langle 110\rangle\|$Si$\langle 110\rangle$ and GaSb$\{002\}\|$Si$\{002\}$.

Figure 5 shows the HRTEM micrographs taken from the GaSb layer grown on the AlSb buffer layer. Just eight 90° misfit dislocations appear in Fig. 5. The driving force for the generation of 90° dislocations is the lattice mismatch between the GaSb layer and the Si substrate. 90° dislocations are the most efficient misfit dislocations for strain relaxation because the length of the Burgers vector edge component projected into the interface b_e is $a/\sqrt{2}$ (the Burgers vector $b_{90°}$ of 90° dislocations is $1/2a\ [\bar{1}\bar{1}0]$). The theoretical average spacing S of 90° misfit dislocations is 3.34 nm because the misfit δ' is about 0.122. However, the 90° misfit dislocations are actually arranged with an average distance of 3.46 nm along the [110] direction in Fig. 5, and eventually there are less 90° dislocations than the theoretical value on the interface between the GaSb layer and Si substrate.

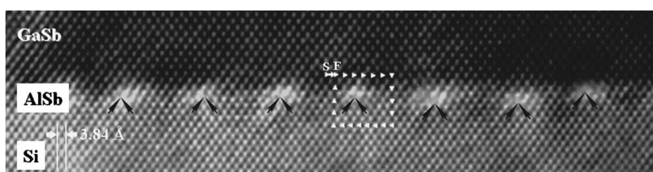

FIG. 5. Cross-sectional HR TEM micrograph for sample B through the [1$\bar{1}$0] zone axis. The arrows indicate 90° dislocations. The Burgers circuit is clockwise according to the start-finish (SF)/right-hand (RH) convention.

In summary, GaSb has been grown to 3D islands and coalesced into bigger islands when they are directly grown on Si substrate. The growth directions have been tilted with the specified orientation relation between GaSb and Si substrate to reduce the lattice misfit. It was observed that tilting of GaSb grains occurred through twin boundaries. The LT AlSb buffer layer plays a key role in the growth of high quality GaSb layer. GaSb layers were epitaxially grown when a LT AlSb buffer was introduced on the interface. Only 90° misfit dislocations, which are the most efficient dislocation for the misfit relaxation, were observed on the interface when the GaSb layer was grown on the LT AlSb buffer.

The work was supported by the Korea Science and Engineering Foundation Research Project No. 10503000169-05M0300-16910 and Terabit Nano Device (TND) of Frontier-21 program sponsored by Korea Ministry of Science and Technology.

[1]E. Alphandery, R. J. Nicholas, N. J. Mason, S. G. Lyapin, and P. C. Klipstein, Phys. Rev. B **65**, 115322 (2002).
[2]F. Hatami, N. N. Ledentsov, M. Grundmann, J. Bohrer, F. Heinrichsdorff, M. Beer, D. Bimberg, S. S. Ruvimov, P. Werner, U. Gosele, J. Heydenreich, U. Richter, S. V. Ivanov, B. Ya Meltser, P. S. Kop'ev, and Zh. I. Alferov, Appl. Phys. Lett. **67**, 656 (1995).
[3]Y. Qiu, D. Uhl, and S. Keo, Appl. Phys. Lett. **84**, 263 (2004).
[4]K. Akahane, N. Yamamoto, S. I. Gozu, and N. Ohtani, J. Cryst. Growth **264**, 21 (2004).
[5]W. K. Liu, J. Winesett, W. Ma, X. Zhang, M. B. Santos, X. M. Fang, and P. J. McCann, J. Appl. Phys. **81**, 1708 (1997).
[6]B. R. Bennett, R. Magno, and B. V. Shanabrook, Appl. Phys. Lett. **68**, 505 (1996).
[7]S. S. Yi, P. D. Moran, X. Zhang, F. Cerrina, J. Carter, H. I. Smith, and T. F. Kuech, Appl. Phys. Lett. **78**, 1358 (2001).
[8]A. G. Milnes and A. Y. Polyakov, Solid-State Electron. **36**, 803 (1993).
[9]G. Motosugi and T. Kagawa, Jpn. J. Appl. Phys. **19**, 2303 (1980).
[10]M. B. Z. Morosini, J. L. Gerrera-Perez, M. S. S. Loural, A. A. G. Vonzuben, A. C. F. da Silveira, and N. B. Patel, IEEE J. Quantum Electron. **QE-29**, 2103 (1993).
[11]O. Hildelbrand, W. Kuebart, K. W. Bnez, and M. H. Pikuhn, IEEE J. Quantum Electron. **QE-17**, 284 (1981).
[12]S. R. Kurtz, R. M. Biefeld, L. R. Dawson, I. J. Fritz, and T. E. Zipperian, Appl. Phys. Lett. **53**, 1961 (1988).
[13]P. T. Staveteig, Y. H. Choi, G. Labeyrie, E. Bigan, and M. Razeghi, Appl. Phys. Lett. **64**, 460 (1994).
[14]K. Segawa, H. Miki, M. Otsubo, and K. Shirata, Electron. Lett. **12**, 124 (1976).
[15]C. Hilsum and H. D. Rees, Electron. Lett. **6**, 277 (1970).
[16]L. Esaki, J. Cryst. Growth **52**, 227 (1981).
[17]L. M. Frass, G. R. Girard, J. E. Avery, B. A. Arau, V. S. Sundaram, A. G. Thompson, and J. M. Gee, J. Appl. Phys. **66**, 3866 (1989).
[18]G. Benz and R. Conradt, Phys. Rev. B **16**, 843 (1977).
[19]G. Balakrishnan, S. Huang, L. R. Dawson, Y.-C. Xin, P. Conlin, and D. L. Huffaker, Appl. Phys. Lett. **86**, 034105 (2005).
[20]G. Balakrishnan, S. Huang, A. Khoshakhlagh, L. R. Dawson, Y.-C. Xin, P. Conlin, and D. L. Huffaker, J. Vac. Sci. Technol. B **23**, 1010 (2005).

Downloaded 21 Apr 2013 to 143.248.118.122. This article is copyrighted as indicated in the abstract. Reuse of AIP content is subject to the terms at: http://apl.aip.org/about/rights_and_permissions